International Journal of Chemical, Materials and Biomolecular Sciences
ISSN: 2415-6620
Vol:8, No:12, 2014

Phenomenological Ductile Fracture Criteria Applied to the Cutting Process

František Šebek, Petr Kubík, Jindřich Petruška, Jiří Hůlka

***Abstract*—**Present study is aimed on the cutting process of circular cross-section rods where the fracture is used to separate one rod into two pieces. Incorporating the phenomenological ductile fracture model into the explicit formulation of finite element method, the process can be analyzed without the necessity of realizing too many real experiments which could be expensive in case of repetitive testing in different conditions. In the present paper, the steel AISI 1045 was examined and the tensile tests of smooth and notched cylindrical bars were conducted together with biaxial testing of the notched tube specimens to calibrate material constants of selected phenomenological ductile fracture models. These were implemented into the Abaqus/Explicit through user subroutine VUMAT and used for cutting process simulation. As the calibration process is based on variables which cannot be obtained directly from experiments, numerical simulations of fracture tests are inevitable part of the calibration. Finally, experiments regarding the cutting process were carried out and predictive capability of selected fracture models is discussed. Concluding remarks then make the summary of gained experience both with the calibration and application of particular ductile fracture criteria.

***Keywords*—**Ductile fracture, phenomenological criteria, cutting process, explicit formulation, AISI 1045 steel.

I. Introduction

THE problem of ductile fracture under monotonic loading as a result of large plastic deformations has been still a great task to researches. Generally, there are four main approaches to the ductile fracture. These are phenomenological criteria, continuum damage mechanics, void nucleation, growth and coalescence and porosity based models. In the present paper, three phenomenological ductile fracture models, namely Xue–Wierzbicki model [1], Extended Mohr–Coulomb criterion [2], and model proposed by Bai and Wierzbicki [3], were chosen and implemented into the commercial finite element code, Abaqus. Such criteria are based on the macroscopic point of view and they are strongly material dependent, therefore there is excessive need of experimental testing to calibrate such models reliably. The experimental program should be managed with care, especially in the case when the models are supposed to cover a wide range of stress states and loading conditions.

Empirical criteria can be applied to various operations as leveling [4] or cutting process. The cutting is one of the most spread technological operation in the industry together with machining, milling, or drilling. In the mass production it is crucial to maintain the process in the most effective way.

F. Šebek, P. Kubík, J. Petruška, J. Hůlka are with the Institute of Solid Mechanics, Mechatronics and Biomechanics, Faculty of Mechanical Engineering, Brno University of Technology, Technická 2896/2, 616 69, Brno, Czech Republic, e-mails: sebek@fme.vutbr.cz, m3petr@gmail.com, petruska@fme.vutbr.cz, hulka@c-box.cz.

II. Calibration process

A. Plasticity

The steel AISI 1045 was used for experimental testing. The plasticity, obeying von Mises yield criterion, was examined through tensile tests of smooth cylindrical specimen. The basic dimensions were 6 mm in diameter and 30 mm gauge length. The test speed was 2 mm/min. There is a multi-linear flow curve in the Fig. 1 estimated using the trial and error method in the sense that the force-displacement curve from numerical simulation was compared to the one from experiment until the satisfying match was reached. In the same figure, there is the flow curve fitted to multi-linear one. It was carried out using the Hollomon's hardening law [5] which takes form

$$\bar{\sigma} = K\bar{\epsilon}^n, \tag{1}$$

where $\bar{\sigma}$ is the equivalent stress, K is the strength coefficient, $\bar{\epsilon}$ is the equivalent strain, and n is the strain hardening exponent. Using the non-linear least square method, the strength coefficient was estimated as 1150 MPa and the strain hardening exponent as 0.30.

Hollomon's hardening law [5] fitted to multi-linear flow curve was used only for estimating the strength coefficient and strain hardening exponent used in all fracture criteria except of model proposed by Bai and Wierzbicki [3]. The multi-linear flow curve was used in all numerical simulations due to its better correlation to the experimental observation.

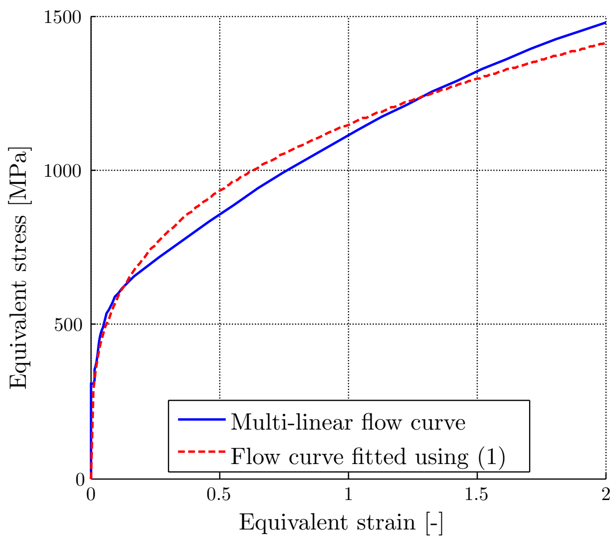

Fig. 1. Multi-linear flow curve and the one fitted using (1)

B. Stress states

The stress state can be characterized by the Cauchy stress tensor $\boldsymbol{\sigma}$ and deviatoric stress tensor $\mathbf{S}$ in form

$$\mathbf{S} = \boldsymbol{\sigma} + p\mathbf{I}, \tag{2}$$

where p is the hydrostatic pressure and $\mathbf{I}$ is the identity matrix.

Using Cauchy stress tensor, the stress triaxiality is

$$\eta = \frac{\mathrm{tr}(\boldsymbol{\sigma})}{3\bar{\sigma}}. \tag{3}$$

Deviatoric stress state can be expressed either by the normalized third invariant of the deviatoric stress tensor as

$$\xi = \frac{27}{2}\frac{\det(\mathbf{S})}{\bar{\sigma}^3}, \tag{4}$$

or, using the previous deviatoric state parameter, by the normalized Lode angle as

$$\bar{\theta} = 1 - \frac{2}{\pi}\arccos(\xi). \tag{5}$$

C. Fracture criteria

As mentioned earlier, fracture tests are inevitable part of ductile fracture criteria calibration. Beside tensile tests of smooth cylindrical specimen, there were conducted tensile tests of notched cylindrical specimens and biaxial tests of notched tube specimen. In the case of notched cylindrical specimens, the diameter in the minimal cross-section area was 6 mm, notch radii were 1.2, 2.5, and 5 mm, and the gauge length was 30 mm. The test speed of quasi-static loading was 2 mm/min. Using biaxial testing of the notched tube specimen, different stress states could be reached by different loading ratios [6]. The quasi-static loading conditions used could be expressed as ratios of an axial and torsional loading components. Ratios -1, -0.5, 0, 0.5, 1, 4.2, and ∞ in mm/rad were chosen.

Next follow criteria to be calibrated. The calibration process was realized with the use of the non-linear least square method. Obtained material constants are listed in Table I. There are fracture envelopes of all criteria shown in Figs. 2-4.

The fracture strain of Xue–Wierzbicki model [1] has form

$$\bar{\epsilon}_f = C_1 \mathrm{e}^{-C_2\eta} - \left(C_1 \mathrm{e}^{-C_2\eta} - C_3 \mathrm{e}^{-C_4\eta}\right)\left(1 - |\xi|^{\frac{1}{n}}\right)^n, \tag{6}$$

where $C_1, \ldots, C_4$ are four material constants.

Extended Mohr–Coulomb criterion [2] has the fracture strain in form

$$\bar{\epsilon}_f = \left[\frac{K}{E_2}\left(\sqrt{\frac{1+E_1^2}{3}}\cos\left(\frac{\pi\bar{\theta}}{6}\right) + \right.\right.$$
$$\left.\left. + E_1\left[\eta + \frac{1}{3}\sin\left(\frac{\pi\bar{\theta}}{6}\right)\right]\right)\right]^{-\frac{1}{n}}, \tag{7}$$

where E_1 and E_2 are two material constants.

The model proposed by Bai and Wierzbicki [3] takes form

$$\bar{\epsilon}_f = \left(\frac{1}{2}\left(D_1 \mathrm{e}^{-D_2\eta} + D_5 \mathrm{e}^{-D_6\eta}\right) - D_3 \mathrm{e}^{-D_4\eta}\right)\bar{\theta}^2 +$$
$$+ \frac{1}{2}\left(D_1 \mathrm{e}^{-D_2\eta} - D_5 \mathrm{e}^{-D_6\eta}\right)\bar{\theta} + D_3 \mathrm{e}^{-D_4\eta}, \tag{8}$$

where $D_1, \ldots, D_6$ are six material constants.

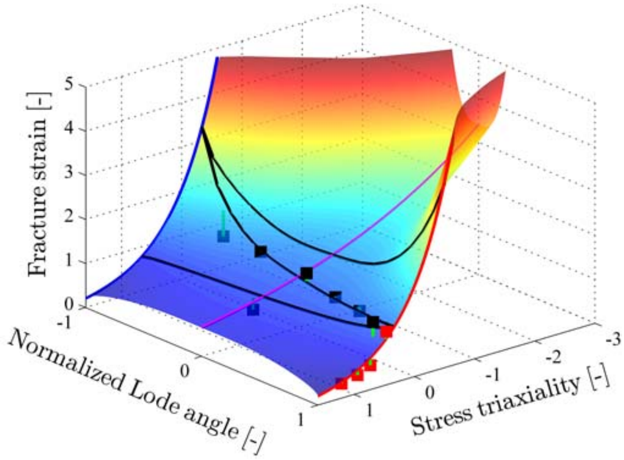

Fig. 2. The fracture envelope of Xue–Wierzbicki model [1]

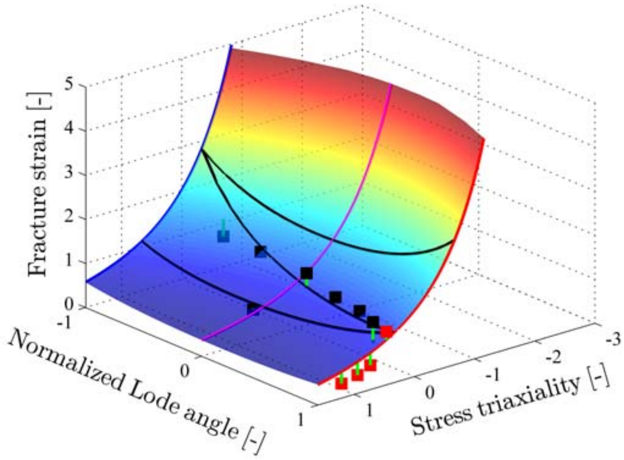

Fig. 3. The fracture envelope of Extended Mohr–Coulomb criterion [2]

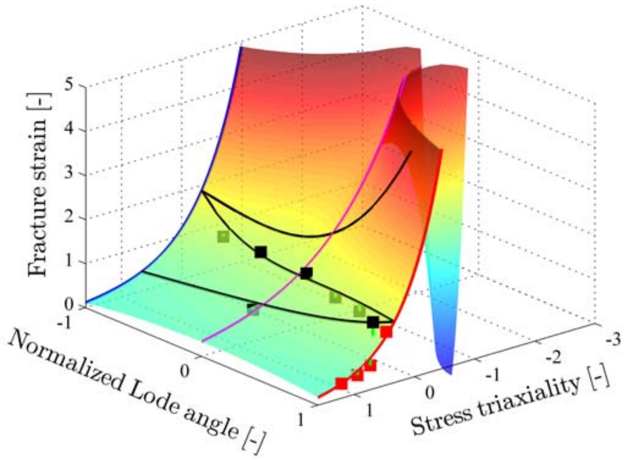

Fig. 4. The fracture envelope of model proposed by Bai and Wierzbicki [3]

In case of model proposed by Bai and Wierzbicki [3], the fracture strain is negative in low stress triaxialities which is unrealistic with improper effect in numerical simulations.

TABLE I
MATERIAL CONSTANTS OF ALL CRITERIA

Xue–Wierzbicki model [1]	Extended Mohr–Coulomb criterion [2]	Model proposed by Bai and Wierzbicki [3]
$C_1 = 2.05$	$E_1 = 0.14$	$D_1 = 2.37$
$C_2 = 1.45$	$E_2 = 683$	$D_2 = 1.63$
$C_3 = 1.15$		$D_3 = 1.20$
$C_4 = 0.36$		$D_4 = 0.81$
		$D_5 = 1.16$
		$D_6 = 1.46$

III. RESULTS AND DISCUSSION

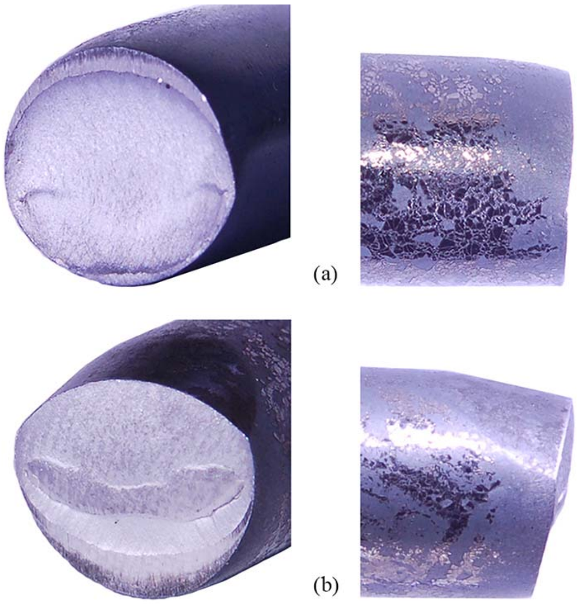

Fig. 5. Fracture surfaces after cutting process experiment for: (a) rod stock; (b) shred [7]

It should be noted that specimens used in cutting process experiments were taken from different block of material than the ones used in calibration fracture tests. There were conducted 10 experiments of the cutting process of circular cross-section rods with 12 mm diameter. The inner diameter of cutting die was 12.55 mm and the diameter of punch was 14.2 mm. The force-displacement curves were filtered and averaged. There are depicted both the rod stock and the shred in Fig. 5.

Using one plane of symmetry, the problem was modeled as a half in the Abaqus software, so the computing time was saved as well as by the mass scaling. There was a negligible ratio of kinetic energy to internal one for whole model. The friction coefficient was applied 0.1 to surfaces in contact.

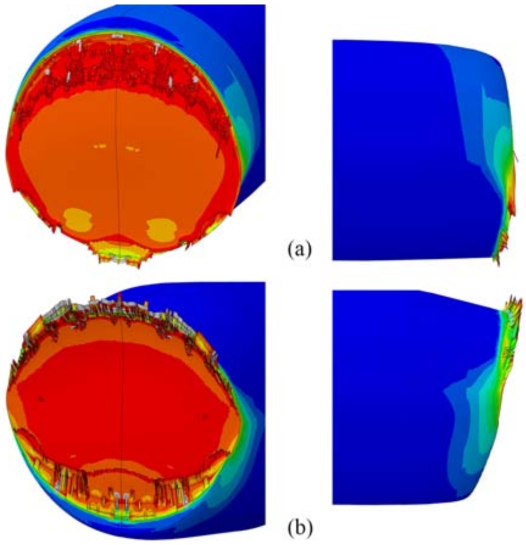

Fig. 7. The damage parameter fields of Extended Mohr–Coulomb criterion [2] after the cutting process simulation for: (a) rod stock; (b) shred

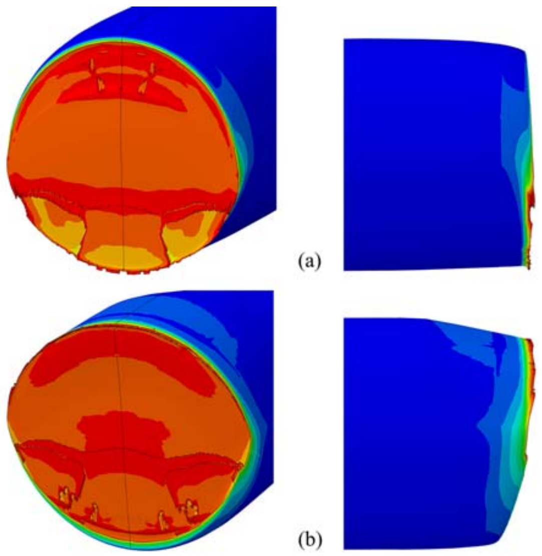

Fig. 6. The damage parameter fields of Xue–Wierzbicki model [1] after the cutting process simulation for: (a) rod stock; (b) shred

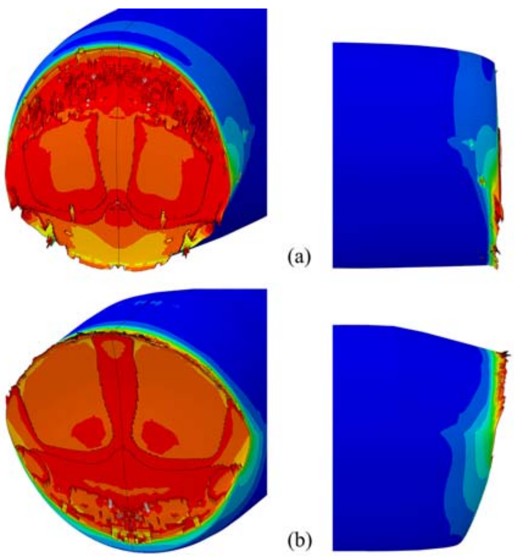

Fig. 8. The damage parameter fields of model proposed by Bai and Wierzbicki [3] after the cutting process simulation for: (a) rod stock; (b) shred

In the process region of meshed rod depicted in Fig. 9, the elements had size 0.075 mm as in numerical simulations of calibration tests. In order to simulate the crack propagation, elements with damage parameter equaling unity were deleted.

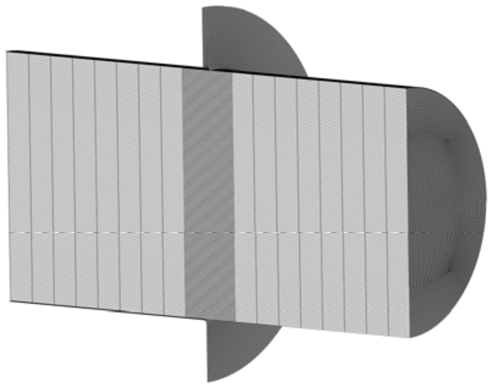

Fig. 9. The discretization of the cutting process simulation

In Figs. 6–8, there are damage parameter fields displayed both on the rod stock and the shred for all ductile fracture criteria. There is no scale of the damage parameter provided, nevertheless the parameter reaches zero when there is no damage (blue color), and it reaches unity when there is ductile fracture initiation (red color). Between these colors, there is a gradual transition (the reader is referred to the electronic version of this paper for references to color). The figures mentioned are particularly intended for comparison between the computationally obtained and experimentally observed fracture surfaces. Visually, the fracture surfaces of rod stock and shred due to numerical simulation using the Xue–Wierzbicki model [1] are the closest to those experimentally observed.

In Fig. 10, there are depicted force-displacement curves both for experiments and numerical simulations. Again, the closest prediction is due to Xue–Wierzbicki model [1]. Among three criteria involved, the model proposed by Bai and Wierzbicki [3] provided the worst prediction.

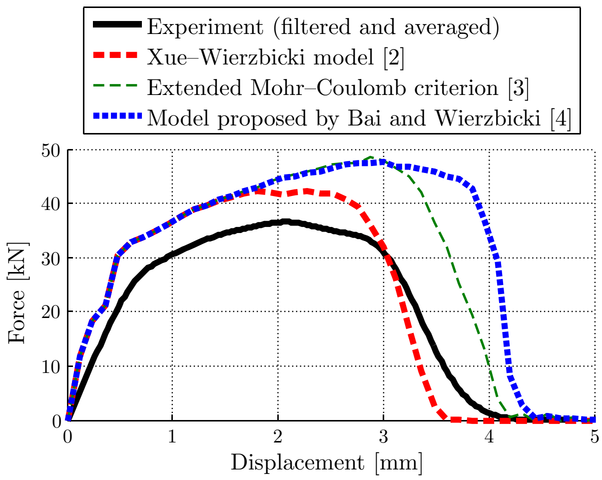

Fig. 10. Force-displacement curves for experiments and simulations

IV. Conclusion

Widely spread technological operation, the cutting process of circular cross-section rods, was carried out experimentally and computationally as well. Three phenomenological ductile fracture criteria were chosen and calibrated using tensile tests of smooth and notched cylindrical specimens together with biaxial tests of notched tube specimen. Their predictive capability and reliability was presented. When summarized, Xue–Wierzbicki model [1] was closest to experimental observation both in the visual comparison of fracture surfaces and in the force-displacement responses. In the scope of our experimental program and chosen ductile fracture criteria, the worst prediction regarding the model proposed by Bai and Wierzbicki [3] can be attributed to poor shape of its fracture envelope in low stress triaxialities. This could be fixed by introducing further experiments situated, naturally, in the region of low stress triaxialities. Unfortunately, the demand on the versatility of ductile fracture criteria is at the expense of complexity.

Future work could be aimed to problems of strain rate and friction. The material behavior alters with the changing strain rate, therefore the optimal cutting speed should be ensured. Moreover, it is crucial to know the friction conditions when performing finite element analysis. Inaccurate values could lead to discrepancies in force-displacement responses when simulating the process either in order to study the operation itself or to find the optimal setup in the perspective of efficiency. All aspects mentioned are directly related to the blunting of the cutting tool leading to the worsening of the quality of fracture surfaces and to raising costs because of the maintaining.

Acknowledgment

This work is an output of cooperation between grant project FSI-S-14-2311 and NETME Centre, regional R&D centre built with the financial support from the Operational Programme Research and Development for Innovations within the project NETME Centre (New Technologies for Mechanical Engineering), Reg. No. CZ.1.05/2.1.00/01.0002 and, in the follow-up sustainability stage, supported through NETME CENTRE PLUS (LO1202) by financial means from the Ministry of Education, Youth and Sports under the “National Sustainability Programme I”.

References

[1] T. Wierzbicki, Y. Bao, Y.-W. Lee, and Y. Bai, “Calibration and evaluation of seven fracture models,” *Int. J. Mech. Sci.*, vol. 47, pp. 719-743, 2005.

[2] Y. Bai, and T. Wierzbicki, “Application of extended Mohr–Coulomb criterion to ductile fracture,” *Int. J. Frac.*, vol. 161, pp. 1-20, 2010.

[3] Y. Bai, and T. Wierzbicki, “A new model of metal plasticity and fracture with pressure and Lode dependence,” *Int. J. Plast.*, vol. 24, pp. 1071-1096, 2008.

[4] J. Petruška, T. Návrat, and F. Šebek, “A new model for fast analysis of leveling process,” *Adv. Mater. Res.*, vol. 586, pp. 389-393, 2012.

[5] J. H. Hollomon, “Tensile deformation,” *Trans. AIME*, vol. 162, pp. 268-290, 1945.

[6] P. Kubík, F. Šebek, J. Petruška, J. Hůlka, J. Růžička, M. Španiel, J. Džugan, and A. Prantl, “Calibration of Selected Ductile Fracture Criteria Using Two Types of Specimens”, *Key Eng. Mater.*, vols. 592-593, pp. 258-261, 2014.

[7] J. Hůlka, *Application of ductile fracture models in computational simulation of manufacturing operations*, Diploma Thesis, Brno University of Technology, 2008.